

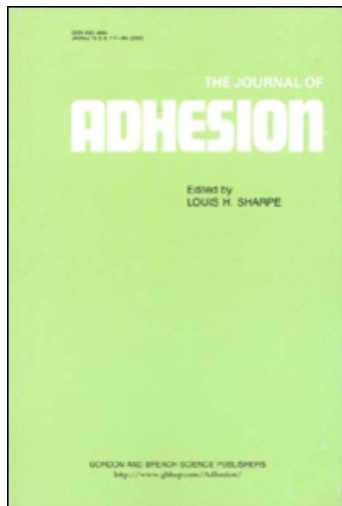
This article was downloaded by:

On: 21 January 2011

Access details: *Access Details: Free Access*

Publisher *Taylor & Francis*

Informa Ltd Registered in England and Wales Registered Number: 1072954 Registered office: Mortimer House, 37-41 Mortimer Street, London W1T 3JH, UK



The Journal of Adhesion

Publication details, including instructions for authors and subscription information:

<http://www.informaworld.com/smpp/title~content=t713453635>

Adhesion at Poly(Butylacrylate)-Poly(Dimethylsiloxane) Interfaces

Nicolas Amouroux^a; Frédéric Restagno^b; Liliane Léger^b

^a ARKEMA K. K., Kyoto Technical Center, Shimogyo-ku, Kyoto, Japan ^b Laboratoire de Physique des Solides, Université Paris sud XI, Orsay Cedex, France

To cite this Article Amouroux, Nicolas , Restagno, Frédéric and Léger, Liliane(2007) 'Adhesion at Poly(Butylacrylate)-Poly(Dimethylsiloxane) Interfaces', The Journal of Adhesion, 83: 8, 741 – 760

To link to this Article: DOI: 10.1080/00218460701585840

URL: <http://dx.doi.org/10.1080/00218460701585840>

PLEASE SCROLL DOWN FOR ARTICLE

Full terms and conditions of use: <http://www.informaworld.com/terms-and-conditions-of-access.pdf>

This article may be used for research, teaching and private study purposes. Any substantial or systematic reproduction, re-distribution, re-selling, loan or sub-licensing, systematic supply or distribution in any form to anyone is expressly forbidden.

The publisher does not give any warranty express or implied or make any representation that the contents will be complete or accurate or up to date. The accuracy of any instructions, formulae and drug doses should be independently verified with primary sources. The publisher shall not be liable for any loss, actions, claims, proceedings, demand or costs or damages whatsoever or howsoever caused arising directly or indirectly in connection with or arising out of the use of this material.

Adhesion at Poly(Butylacrylate)–Poly(Dimethylsiloxane) Interfaces

Nicolas Amouroux

ARKEMA K. K., Kyoto Technical Center, Shimogyo-ku, Kyoto, Japan

Frédéric Restagno

Liliane Léger

Laboratoire de Physique des Solides, Université Paris sud XI,
Orsay Cedex, France

We present an investigation of the adhesion modulation mechanisms of silica-like nanoparticles (MQ resins) incorporated in polydimethylsiloxane (PDMS) elastomers and acrylic adhesives. The Johnson-Kendall-Roberts (JKR) test has been used to gain information on the both zero velocity and the velocity dependence of the adhesive strength, avoiding as much as possible contributions to the adhesive strength of bulk dissipation in the adhesive (which is not the case with peel tests). As the incorporation of the MQ resins into the elastomers deeply affects their own mechanical properties, the loading and unloading curves of small poly(butylacrylate) (PBA) lenses on either PDMS elastomers, adsorbed PDMS and pure MQ resin layers are compared in a systematic manner. The PBA chains are observed to have a neat affinity for the MQ resin nanoparticles. When MQ resins are present at the interface, they tend to prevent fracture propagation, thus producing a larger deformation of the PBA lens. The modulation of adhesion is then dominated by the corresponding dissipation inside the acrylic adhesive.

Keywords: Acrylic adhesives; Adhesion mechanisms; Dissipation; Interfacial interactions; JKR test; Modulation of adhesion; Silicone elastomers

Received 25 June 2007; in final form 14 July 2007.

One of a Collection of papers honoring Liliane Léger, the recipient in February 2007 of *The Adhesion Society Award for Excellence in Adhesion Science, Sponsored by 3M*.

Address correspondence to Liliane Léger, Laboratoire de Physique des Solides, UMR 8502 CNRS–Université Paris Sud XI, Batiment 510, F-91405 Orsay Cedex, France. E-mail: leger@lps.u-psud.fr

INTRODUCTION

In two preceding papers [1,2], we have started to describe a systematic investigation of the role of small silica-like nanoparticles named MQ resins in the modulation of adhesion at polydimethylsiloxane (PDMS) elastomers—acrylic adhesive interfaces through the so called JKR test [3]. In a first approach, in order to trace back the role of the incorporation of the MQ resins into the silicon elastomer, we have analyzed the formation and rupture of contact between small PDMS elastomer lenses put into contact with a thin layer of acrylic adhesive (typical thickness 30 nm) deposited on a silicon wafer [1]. This thickness of the adhesive layer was kept nanometric in order to insure that no important dissipation could take place inside the adhesive during the pull off process. Varying, in a systematic manner, the resin content in the elastomer, we could thus demonstrate that the MQ resins were playing a marginal role on the thermodynamic work of adhesion, but were able to greatly affect the velocity dependences of the adhesive strength of these interfaces, in a way which strongly depended upon the time of contact. In order to better understand these effects, systematic experiments on model surfaces were conducted with the same PDMS elastomer lenses containing various amounts of MQ resins, but now put into contact with silicon wafers covered with self assembled monolayers of thiol molecules, with varying amounts of carboxylic extremities [2]. On such layers, again measuring the adhesive strength of the interface as a function of the MQ resin content, of the COOH content in the surface layer, and of both the contact time and the velocity of the fracture, we were able to put into evidence two competing effects: increasing the MQ resin content in the elastomer leads to increased interactions at the interface resulting from the increased polarity of the elastomer lens. However, at the same time, increasing the MQ resin content in the elastomer changes its mechanical properties, increasing its elastic modulus and increasing its viscoelastic response in a more important manner. The mobility of the chains close to the interface is thus decreased as a result of the incorporation of the MQ resin into the network, and it takes a much longer contact time to reach a given level of adhesion. Then, one not only needs MQ resins to be present close to the interface to produce enhanced adhesion, but these MQ resins also need to be sufficiently mobile to be able to find an interaction site in a reasonable time, in order to act as adhesion promoters. We present here the third part of this investigation, with a system now closer to the applied situation, with thick acrylic adhesive in contact with thick antiadhesive PDMS elastomer layers containing various amounts of MQ resins. In order to

fully characterize the adhesive behavior of these systems, the JKR test is used in a systematic manner, with now small elastomer lenses made of crosslinked butylacrylate (BA) and put into contact with 1 mm thick flat layers of PDMS elastomers deposited on silicon wafers. Results for both loading and unloading experiments will be presented and compared with similar experiments performed with the same BA lenses put into contact with a layer of pure PDMS adsorbed on a silicon wafer, or a layer of pure MQ resin also adsorbed on a silicon wafer.

MATERIALS AND METHODS

Both the home-made JKR apparatus and the physico-chemical characteristics of the PDMS elastomers with or without MQ resins have already been described [1,2]. We only detail here the formation of the BA lenses used.

Sample Preparation

The BA micro-lenses were formed by crosslinking poly(*n*-butylacrylate) (PnBA, Sigma-Aldrich, Lyon, France; $M_n = 20$ kg/mol, $M_w = 60$ kg/mol). The glass transition temperature is $T_g = -54^\circ\text{C}$ [4] and its surface energy is $\gamma = 33.7$ mJ/m² at 20°C [5].

The crosslinking procedure was chosen following the protocol described by Anh and Shull [4–6]: dicumyl-peroxide (DCP) was added to a 50% by weight solution of PBA in toluene. The quantity of DCP was calculated to be equivalent, in terms of number per polymer chain to that used by Anh and Shull, *i.e.*, 25% of the total mass of polymer used. Small drops of the solution were deposited on a perfluorinated glass slide, and heated at 150°C for 3 hours, in a reactor under dry nitrogen. Then the small lenses were fully dried in a vacuum chamber for 24 hours, in order to extract all volatile products. They were then used without any further extraction or rinsing procedure.

The PDMS elastomer layers, with or without MQ resins, were cross-linked through the procedure described in [1], at the optimum ratio of SiH over vinyl termination determined for the chosen quantity of MQ resins, in the presence of Karstedt catalyst. Flat 1 mm thick layers were obtained by coating a clean glass slide with the uncrosslinked mixture, under dry atmosphere inside a glove box, and at low enough temperature in order to prevent the beginning of the crosslinking reaction. When the coating layer was flat enough, the temperature was increased to allow for the crosslinking. After curing, these elastomer layers were extracted in a large amount of toluene for nine days,

and finally rinsed in a solution of dodecanethiol in toluene, in order to kill any remaining catalyst.

The PDMS thin adsorbed layer was formed by incubating a clean silicon wafer with α - ω -OH terminated PDMS melt, molecular weight $M_w = 105$ kg/mol (polydispersity index $I = 1.1$). After one night at 100°C , all unattached PDMS molecules were rinsed away. The thickness of the remaining dry PDMS layer was found to be 18 nm, which corresponds to the thickness for a dense adsorbed layer from a melt for that molecular weight [7].

The adsorbed layer of pure resin was obtained by spin coating a solution of MQ resin in xylene, (5% by weight) on a silicon wafer previously cleaned by a UV-ozone treatment [8]. After drying, a layer of MQ resin with a thickness of 150 nm as measured by ellipsometry was obtained, with a typical surface roughness of 1 nm. This layer is not very robust, and is destroyed by rubbing or by rinsing with solvent.

Measurement Protocol

The PnBA micro-lenses formed are much more sticky than the PDMS lenses. We have, thus, used the JKR test under dynamic unloading cycles, in a way quite similar to what is done in a probe tack experiment, and similarly to what has been reported by Anh *et al.* [4–6]. This allows one to control the velocity range investigated.

The protocol used was as follows:

- Loading up to a chosen contact area by small successive displacements of a few micrometers.
- Unloading, after a given time under maximum load, at chosen unloading velocity in the range 0.05 – 5 $\mu\text{m/s}$. The waiting times under load were chosen in the range 15–30 mn.

LOADING EXPERIMENTS: ELASTIC MODULUS AND THERMODYNAMIC WORK OF ADHESION

PnBA Lenses in Contact with Rigid Substrates

Loading curves in terms of normalized load *versus* normalized radius of the contact area [1] are presented for two different loading velocities in Figure 1, for a PnBA lens in contact with a thin adsorbed layer of PDMS. The work of adhesion, W , deduced from the JKR analysis of these curves appears to depend on the loading rate. It increases from 60 to 80 mJ/m^2 when the loading velocity is decreased from 3.3×10^{-2} to 6×10^{-4} $\mu\text{m/s}$ (*cf.* Figure 1). Similar trends have been observed for

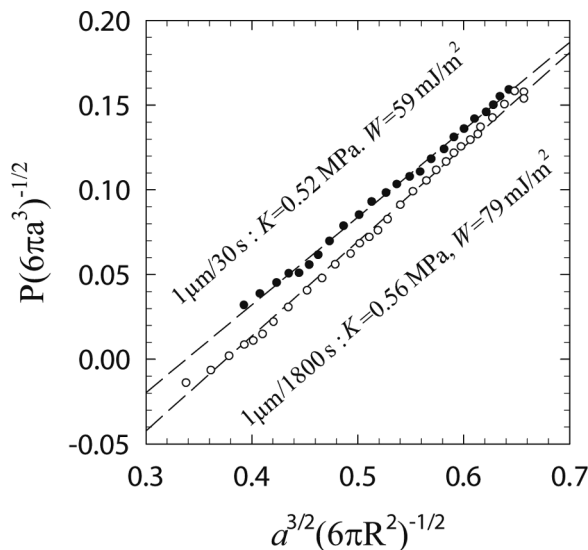


FIGURE 1 Loading curves in terms of normalized load as a function of the normalized radius of contact for PBA lenses in contact with PDMS, for two different loading velocities.

the contact on the adsorbed MQ resin layer. The elastic modulus, $K = 0.55 \pm 0.05$ MPa, is smaller than that of the softer PDMS elastomer used in the present investigation (1 MPa).

PnBA Lenses in Contact with Elastomer Layers

Similar experiments conducted in the case of a contact between PnBA lenses and thick elastomer layers show, as in Figure 1, a linear relation between the normalized load and the normalized radius of the contact area. This is a proof that the JKR approach correctly describes the loading process. This also allows one to deduce an effective modulus of the system, as now both sides of the contact have a finite elastic modulus. Figure 2 shows a comparison between the values of this effective elastic modulus on PDMS layers with various MQ resin contents and that calculated through $K^{-1} = K_{PBA}^{-1} + K_{PDMS}^{-1}$, using the values deduced from Figure 1 for K_{PBA}^{-1} and those from [1] for K_{PDMS}^{-1} with the various MQ contents.

The PnBA lenses thus appear softer than all PDMS layers used. Thus, they will be the more deformed partner of the assembly under loading. Concerning the values of the thermodynamic work of adhesion, the order of magnitude is as expected, ($W = 54$ mJ/m² for

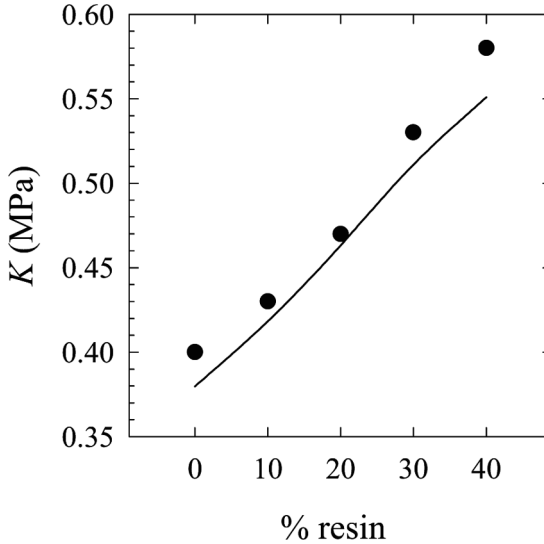


FIGURE 2 Rigidity constants, K , measured for PBA lenses in contact with PDMS elastomers containing various amounts of MQ resins. The line corresponds to the expected values, inverse of the sum of the respective compliances of the PBA and the elastomer.

PDMS/PnBA), but the observed velocity dependences are indicative of viscoelastic contributions.

UNLOADING EXPERIMENTS

Rough Results

In Figures 3 and 4, we have reported the evolution of the radius of the contact area, a , as a function of the load, for both the loading and the unloading steps of the experiment, for various unloading velocities, and for, respectively, the contact of PnBA lenses–PDMS layers (Figure 3) or PnBA lenses–MQ resin layers (Figure 4).

The adhesive strength appears much larger in the case of the MQ resin layer than in the case of PDMS, as evidenced by the much larger hysteresis in the JKR curves.

Analysis of a Loading-Unloading Cycle for a Contact with MQ Resin Layer

Loading and unloading curves for a PnBA lens in contact with an adsorbed layer of MQ resin, at the unloading velocity of $1 \mu\text{m/s}$, are

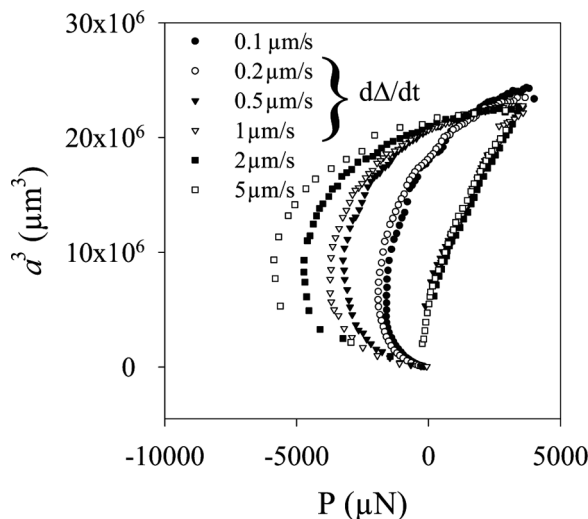


FIGURE 3 Loading and unloading curves with various imposed unloading velocities for PBA lenses in contact with an adsorbed PDMS layer.

reported in Figure 5, in terms of radius of the contact area as a function of the load (Curve 5a) and deformation in the centre of the contact as a function of the contact radius (Curve 5b). The radius of the lens is

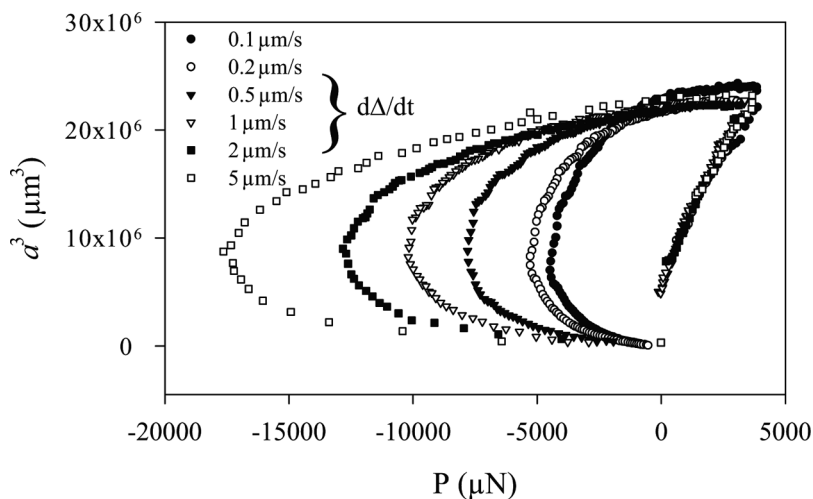


FIGURE 4 Loading and unloading curves with various imposed unloading velocities for PBA lenses in contact with an adsorbed resin layer.

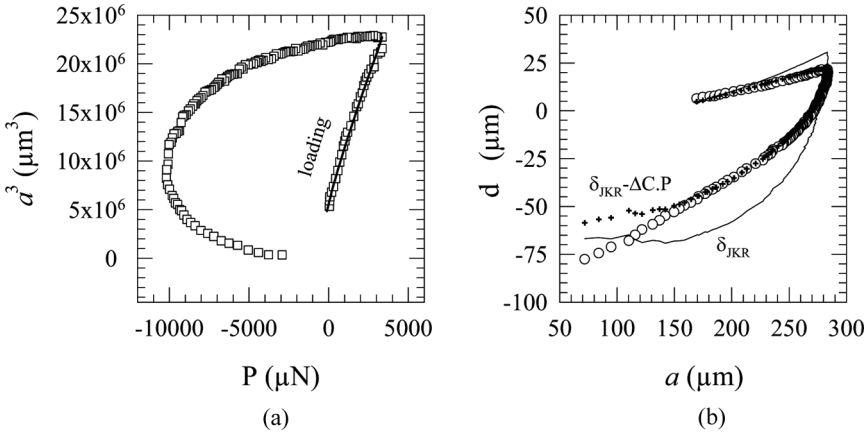


FIGURE 5 Loading-unloading cycle for a PBA lens in contact with an adsorbed layer of resin.

$R = 1750 \mu\text{m}$, and its maximum height is $h = 700 \mu\text{m}$. The solid line in Figure 5b represents the JKR curve adjusted to the loading part of the curve, without taking into account any finite size effects [4,9]. The crosses represent the calculated JKR curve including finite size effects [4,9] and adjusted to the loading part of the curve. The best fitted curve leads to a correction of the compliance, due to finite size effects $\Delta C = 2.17 \text{ mN/m}$, quite close to the expected value $8/(3\pi Kh) = 2.33 \text{ mN/m}$ [10]. The JKR description of the contact, thus, well describes both the loading and the unloading steps, provided one includes finite size corrections, except at the end of the unloading for which one can clearly see in Figure 5b that a deviation appears between calculated JKR and measured points, below a limiting contact radius $a_1 = 170 \mu\text{m}$. This means that, for such final unloading steps, the displacements are no longer elastic, and the JKR mechanics no longer holds.

In Figure 6, we have reported $G(V)$ curves calculated from the data of Figure 5a, for contact radius larger than the limiting radius $a_1 = 170 \mu\text{m}$. The curve $G(V)$ presents an abrupt step for $V_c = 0.3 \mu\text{m/s}$. Three velocity regimes can be identified:

- $V > V_c$: $G(V)$ can be described by a power law, with an exponent 0.64.
- $V = V_c$: G evolves from 200 to 350 mJ/m^2 at fixed velocity, and the radius of contact is $a_c = 270 \mu\text{m}$ at this point.

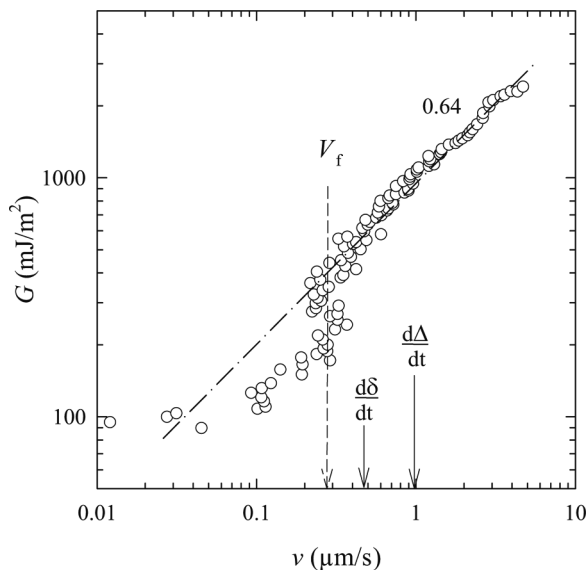


FIGURE 6 Evolution of the adhesive strength, G , as a function of the velocity of the fracture, V , obtained when unloading a PBA lens in contact with an adsorbed resin layer, the unloading imposed velocity is $d\Delta/dt = 1 \mu\text{m/s}$.

- $V < V_c$: the curve remains below that obtained by extrapolating the high velocity regime, meaning that to reach a given G , one needs a higher velocity than what would have been necessary if the high velocity regime had covered the whole velocity range.

Curves similar to Figure 6 have been obtained with all substrates, whatever the imposed velocity. The critical velocity, V_c , has been observed to depend only on the vertical pulling velocity of the microlens, $d\delta/dt$. In fact, the experimental procedure imposes $d\Delta/dt = 1 \mu\text{m/s}$. However, due to the finite rigidity of the force sensor which partly follows the displacement, the real displacement velocity, $d\delta/dt$, differs from the imposed pulling velocity, $d\Delta/dt$. At the beginning of the unloading $d\delta/dt$ remains constant, and for the data presented in Figure 6, $d\delta/dt = 0.45 \mu\text{m/s}$. Then, for large pulling displacements, $d\delta/dt$ no longer remains a constant, as will be demonstrated by the direct observations presented below. As above V_c the behaviour of the unloading appears “classical,” one can in a first step compare the $G(V)$ curves obtained on the different substrates restricting the investigations with the “normal” high velocity part of the curves.

G(V) CURVES

In a first approach, we restrict the analysis to the velocity range above V_c , and compare the observed velocity dependence of the adhesive strength, G , of PnBA lenses on the different substrates used.

Figure 7 presents the results obtained on both the PDMS and the MQ resin adsorbed layers. Power law dependences are obtained, with a larger slope on the MQ resin than on the PDMS layer.

In Figure 8, we have reported the results obtained for a PnBA lens in contact with PDMS elastomers containing various amounts of MQ resins. Again, power laws are obtained, but, surprisingly, the exponent seems to be independent on the resin content in the elastomer.

As shown in Figure 9, all curves form a unique master curve when reported in scaled units $G - G_0/G_0 = \phi(V)$, thus defining a unique dissipation function, $\phi(V)$. The data in Figure 9 yield $\phi(V) = (V/V^*)^n$ with $n = 0.4 \pm 0.03$. It is worth noticing that on the PDMS adsorbed thin layer, exactly the same dissipation function is obtained. Similarly, on both adsorbed MQ resin layers and PDMS thin films, master curves can be formed as shown in Figure 10. All characteristic parameters of the $G(V)$ curves extracted from such an analysis are gathered in Table 1 for PDMS elastomer containing various amounts of MQ resins,

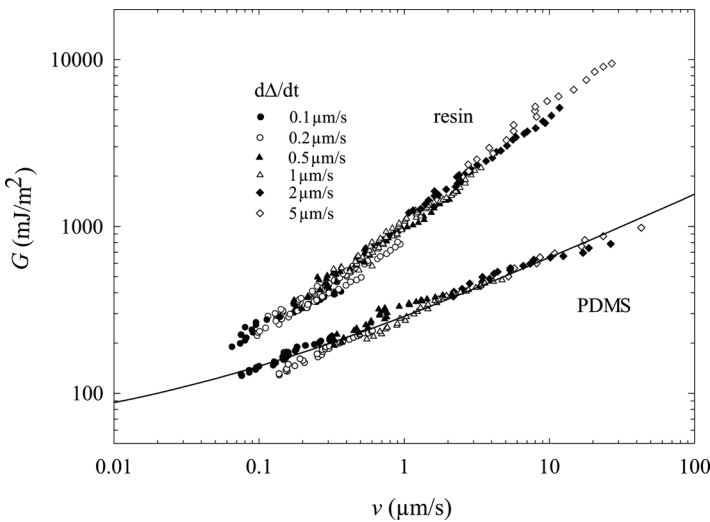


FIGURE 7 Master curves obtained for the adhesive strength as a function of the unloading velocity, when comparing all unloading curves for PBA lenses in contact with either an adsorbed PDMS layer or an adsorbed resin layer.

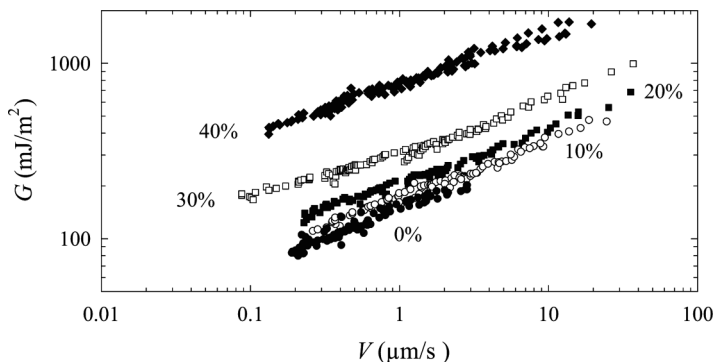


FIGURE 8 Master curves for the adhesive strength as a function of unloading velocity, obtained when comparing all unloading curves for PBA lenses in contact with PDMS elastomers containing various amount of MQ resins.

PDMS-adsorbed layer, and MQ resin adsorbed layer as substrates, against comparable PnBA micro-lenses. As shown in Figure 11, on elastomer substrates, G_0 is observed to slowly increase with the resin content up to 20%, and then to strongly increase nonlinearly above 20% of MQ resin. All parameters in Table 1 are moderately affected by the time of contact spent under maximum load before unloading, as exemplified by the data for $G(V)$ as a function of contact time reported in Figure 12 for PnBA lenses in contact with either adsorbed MQ resin layers or PDMS layers.

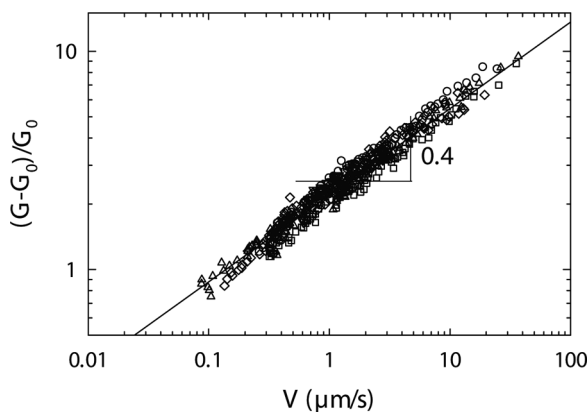


FIGURE 9 Unique dissipation function for PBA lenses in contact with PDMS elastomers with various amounts of MQ resins.

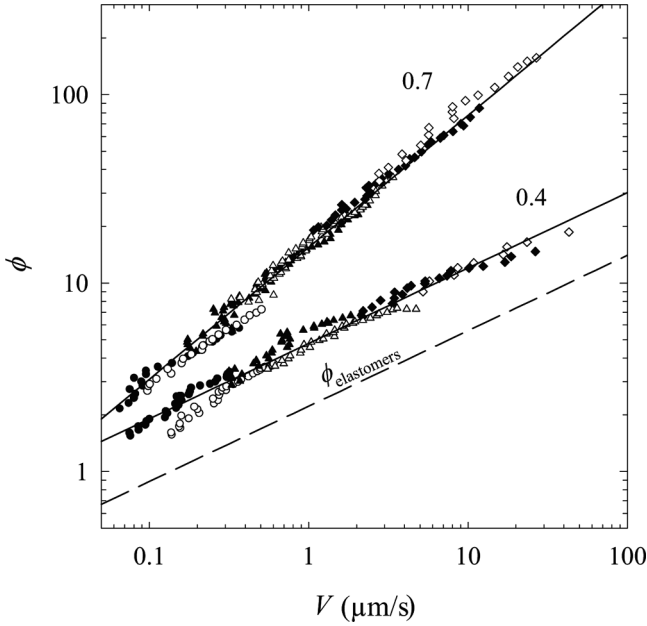


FIGURE 10 Dissipation functions for PBA lenses in contact with adsorbed resins and adsorbed PDMS layers. The dissipation function on the PDMS elastomers (dotted line, data from Figure 9) is also reported for comparison.

TABLE 1 Values of the Parameters G_0 , V^* and n Obtained When Gathering All Data Obtained for the Adhesive Energy of PBA Lenses in Contact with PDMS Elastomers Containing Various Amounts of MQ Resins as a Function of the Fracture Velocity V , to Form the Master Curve of Figure 9, Along with Similar Parameters for Either PBA Lenses on Pure PDMS or Pure MQ Adsorbed Layers

Substrate	G_0 (mJ/m ²)	V^* (μm/s)	n
Elastomer 0%	45 ± 5	0.135 ± 0.07	0.4 ± 0.03
Elastomer 10%	50 ± 5		
Elastomer 20%	60 ± 5		
Elastomer 30%	95 ± 7		
Elastomer 40%	220 ± 10		
Adsorbed PDMS	50 ± 10	0.020 ± 0.010	
Adsorbed Resin	60 ± 10		0.7 ± 0.05

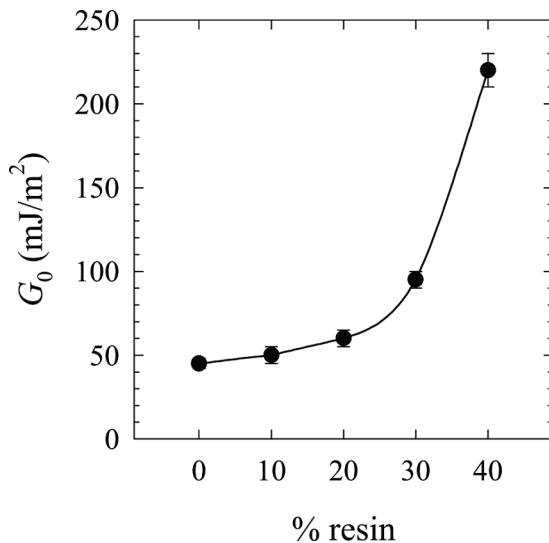


FIGURE 11 Values of the adhesive strength extrapolated at zero velocity, G_0 , used to form the master curve of Figure 9, as a function of the MQ resin content in the elastomer.

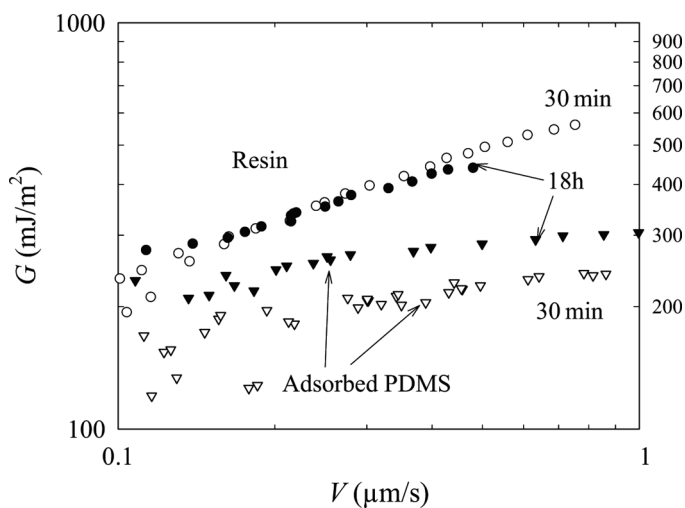


FIGURE 12 Effect of the contact time under load between the PBA lenses and the substrate (either adsorbed PDMS layer or adsorbed resin layer) on the velocity dependence of the adhesive strength, $G(V)$.

OBSERVATION OF THE DEFORMATION OF THE PnBA LENSES DURING UNLOADING

We have optically monitored the deformations of the PnBA micro-lenses during unloading through two CCD cameras, one observing the contact from the top, and the second one observing the contact laterally, both through an optical long distance microscope (Questar, New Hope, PA, USA; working distance 20 cm). We first analyse below the beginning of the unloading. Then we shall present images showing the destabilization of the contact line between the lens and the substrate at higher pulling distance; finally, we shall discuss lateral views of the lens which allow one to analyse the angle at which the lens connects to the substrate (contact angle).

Anchoring of the Lens on the Substrate

Observing the series of pictures of the top view of the contact upon unloading (Figure 13), one can easily observe that, at a given time during the unloading, a second line appears in the images, which remains

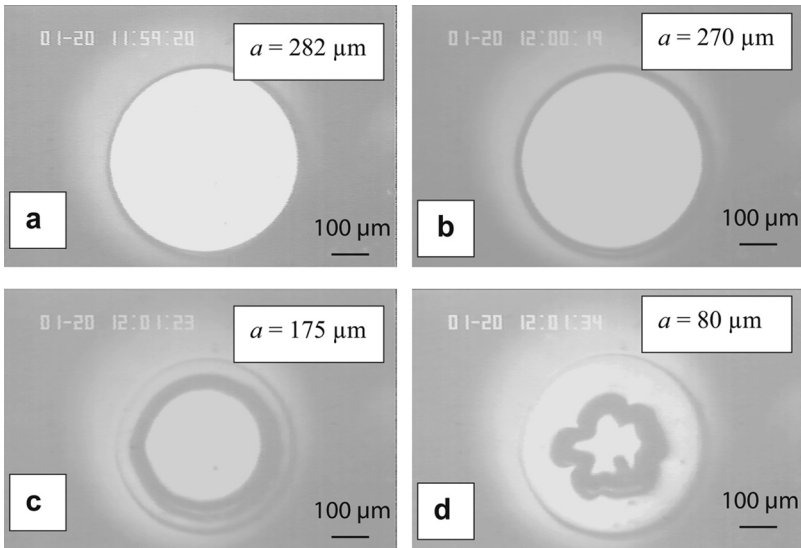


FIGURE 13 Series of top view of the contact (through the lens) showing the evolution of the contact between a PBA lens and an adsorbed resin layer, and an unloading velocity $d\Delta/dt = 1 \mu\text{m/s}$. One can notice the radius of contact on the second picture (13b) identical to the radius of the rim in picture 13c.

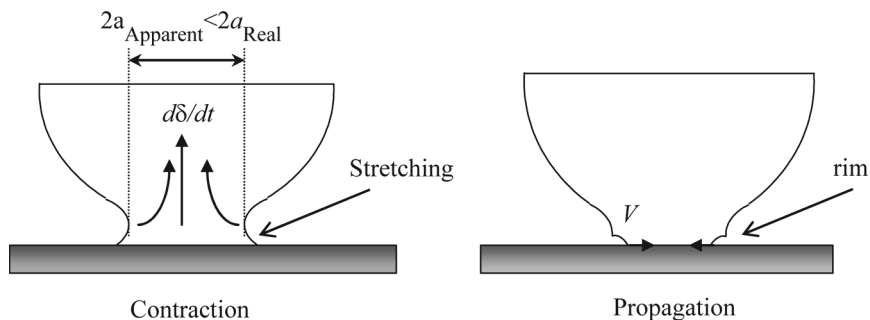


FIGURE 14 Schematic representation of the evolution of the contact and of the deformation of the PBA lens during unloading. When the fracture starts to propagate, a rim remains on the lens, visible as the second circular line in pictures c and d in Figure 13.

almost immobile, while the radius of the contact area decreases. This is particularly clear in Figure 13c with the thick dark line indicating the contact area and the thin black larger circle being this second feature. It arises from a deformation of the lens as schematically presented in Figure 14. This deformation relaxes back very slowly and the lens recovers its smooth shape if one waits typically 15 min. This deformation appears whatever the substrate and whatever the unloading velocity chosen. Its radius, $270\ \mu\text{m}$, is equal to a_c , defined as the limit at which the “normal” high velocity behaviour starts.

We can, thus, propose the following interpretation for all observations reported above and the shape of the $G(V)$ curves: when starting to unload, the velocity of the contact line is small and G is close to W . When pulled at constant velocity, the soft lens deforms while the fracture remains almost immobile (Figures 13a and 13b). When G becomes bigger than $G(V_c)$ ($350\ \text{mJ}/\text{m}^2$ in the example described above) the velocity of the fracture increases. There is a real propagation of the fracture, with the velocity $V = -da/dt$ which corresponds to a real detachment of the foot of the lens from the substrate (Figure 14). To summarize: we impose a pulling velocity $V_c = d\delta/dt$ to the system, but the fracture is only initiated when G becomes larger than G_c . The initially observed contraction results from the softness of the lens and possibly the substrate.

Destabilization of the Contact Line

The destabilization of the contact line shown in Figure 13d is only observed on elastomer substrates with MQ resin in the range of

velocities we have investigated. This is illustrated in Figure 15 where images of the contact are reported at similar velocities and similar unloading times for a lens on pure MQ resin and on adsorbed PDMS layers.

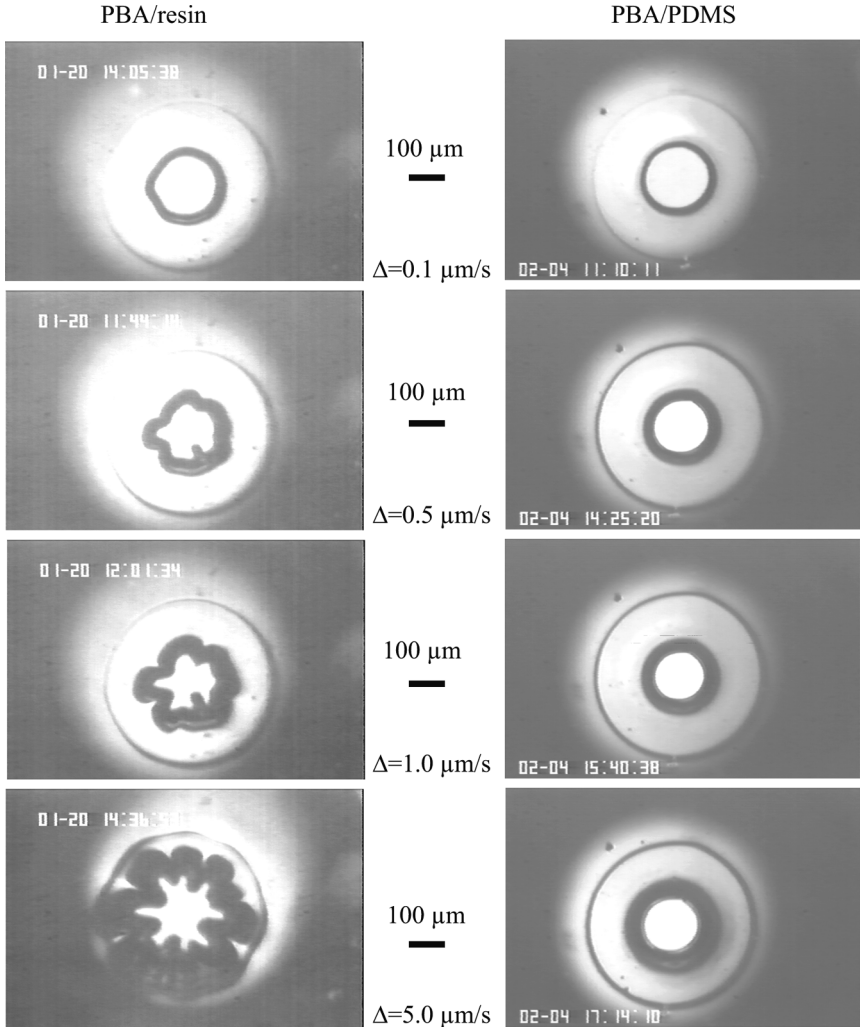


FIGURE 15 Evolution of the contact lines during unloading for PBA lenses in contact with an adsorbed layer of resin or an adsorbed layer of PDMS. For comparable upward displacements, the contact is clearly smaller on PDMS than on resin, and the contact line becomes distorted and destabilized much sooner on the resin layer than on PDMS.

Lateral View of the Contact

From the lateral observation (not shown here) of the contact between the PnBA microlenses and the various substrates (pure adsorbed resin layer, pure PDMS layer or elastomers containing various amounts of MQ resins) one can immediately see that PnBA lenses tend to de-wet from the resin (the contact angle between the lens and the substrate is close to 90°), while it wets the PDMS (and the situation is intermediate on PDMS elastomers with MQ resin). At the same time, the final stages of the decompression correspond to contact areas as small as $15\ \mu\text{m}$ in radius, and quite large vertical displacements ($50\ \mu\text{m}$): the PnBA is strongly elongated and forms a long fibril.

Analysis in Terms of “Tack” Experiment

Analogous strong destabilizations of the contact along with fibril formation are often observed when pressure sensitive adhesives are tested through peel or probe tack tests. The JKR mechanical analysis of the contact obviously cannot be applied to describe these large deformations. Instead, the total work for a loading-unloading cycle can be calculated from the simultaneous measurements of the load, P , and of the displacement, δ . The corresponding energy per unit area, normalized by the maximum contact area is $T = 1/\pi a_{\text{max}}^2 \oint P d\delta$.

The data for T as a function of the pull velocity $d\Delta/dt$ are reported in Figure 16 for PnBA lenses in contact with adsorbed resin and PDMS layers. Power laws are observed, with exponents comparing quite well with what has been obtained with the JKR analysis (Figure 10). In order to get such a result, one needs to keep in mind that using a JKR machine as a probe tack-like test may be delicate, due to the compliance of the machine. In the present experiments, we have taken care to always use the same JKR machine, and to always load up to the same maximum contact area. Then, the JKR cycle essentially captures the dissipation contribution to the adhesive strength of the contact, even if the real velocity of the contact line, da/dt , differs from the pull velocity, $d\Delta/dt$.

Localization of the Fracture Plane

As can be inferred from a direct observation of the adsorbed resin layer after the rupture of the contact, the fracture is clearly cohesive on such substrates: Figure 17 shows an observation of the substrate, by optical microscopy in polarized reflected light: the clear disc corresponds to the contact area at the beginning of the unloading. The contrast allows

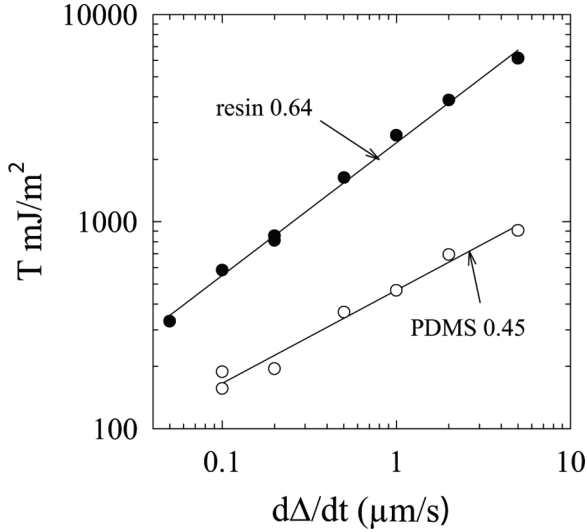


FIGURE 16 Analysis of the energy dissipated during the loading-unloading cycle for the contact between PBA lenses on either an adsorbed resin or PDMS layers as a function of unloading rate, similar to what is usually done for a probe tack test.

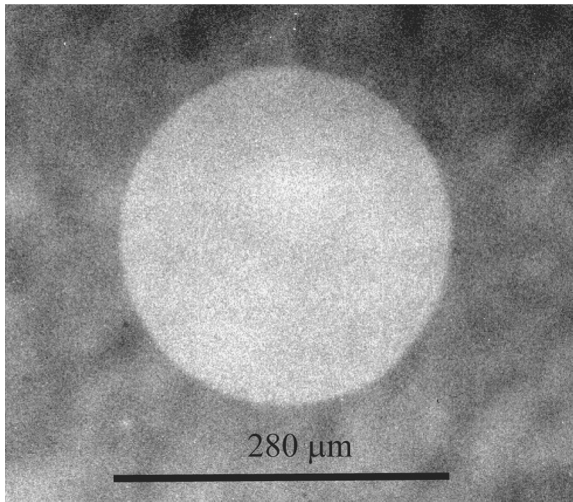


FIGURE 17 Image, through an optical microscope in reflected polarized light, of the adsorbed resin layer after rupture of the contact with a PBA lens. Radius of the contact disc: 280 μm .

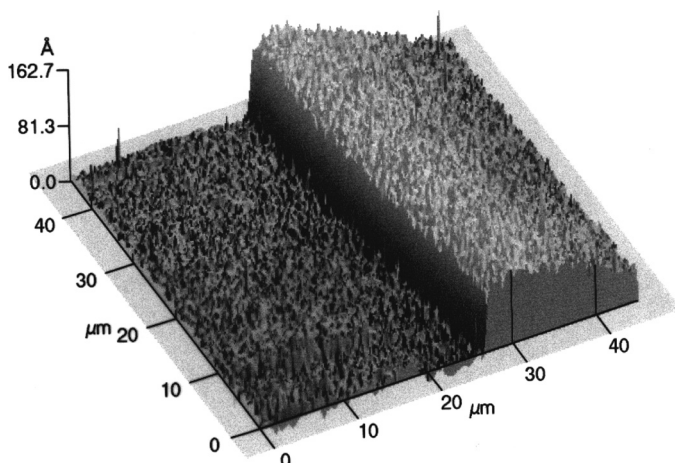


FIGURE 18 Three dimensional view of the edge of the contact between a PBA lens and an adsorbed MQ resin layer after rupture, as seen in non-contact AFM. A 15 nm thick PBA layer remains on the substrate, indicating a cohesive failure.

one to say that there is a difference in thickness of the adsorbed resin layer of approximately 15 nm. The central part (contact) is indeed at a upper level than the outer surface of the adsorbed resin layer, as shown by the atomic force microscopy (AFM) image of the edge of the contact line in Figure 18.

On PDMS layers, we have not been able to determine any change in thickness at the location of the contact (even through microbeam ellipsometry) probably indicating an adhesive fracture.

CONCLUSION

All above-reported features show that contrary to what had been observed when the thickness of the acrylic adhesive was kept very small, the modulation of adhesion for contacts between a thick acrylic adhesive and various PDMS elastomers containing MQ resins as adhesion modulators, is dominated by dissipation inside the adhesive layer: the dissipation functions characteristic of the rupture of these contacts do not depend on the amount of MQ resin inside the PDMS elastomer. Increasing the viscoelasticity of the elastomer by increasing the MQ resin content is not the major factor which changes the adhesive strength.

The adhesive energy at zero velocity of the fracture does depend on the MQ resin content in the elastomer, and increases with this MQ

content, in a non-linear manner. This increased adhesion is further amplified through the velocity dependence of the dissipation function when the fracture propagates at finite velocity.

The precise role played by the MQ resin at the interface is not fully elucidated. The investigation of the contact between the PnBA lenses and an adsorbed layer of pure resin gives, however, some important indications: on this pure resin layer, the rupture of the contact is cohesive. The resin layer is thus able to trap some PnBA chains, even after a short contact time. On pure elastomers without MQ resin the fracture is adhesive. On elastomers with a large amount of MQ resin, we cannot definitively conclude at present the location of the fracture and it may be at least partly cohesive. If one admits that the MQ resin particles close to the interface are able to rapidly attract PnBA chains when the contact is formed, it is plausible to admit that the observed increase in G_0 is due either to an extraction process of these PnBA chains attached to the elastomer surface from the PnBA lens or to a fracture of these chains attached to the surface through a Lake and Thomas mechanism [11].

Finally, we have shown that the way the PnBA lens “dewets” the substrate depends on the composition of this substrate in MQ resins: the MQ resin seems to slow down fracture and prevent the PnBA from leaving the contact with the substrate. As the PnBA lens is then highly deformed, one needs take into account the shear components of the deformation field inside the adhesive to fully account for the observed dissipation functions.

REFERENCES

- [1] Léger, L. and Amouroux, N., *J. Adhesion* **81**, 1075–1099 (2005).
- [2] Amouroux, N. and Léger, L., *J. Adhesion* **82**, 919–932 (2006).
- [3] Johnson, K. L., Kendall, K., and Roberts, A. D., *Proc. R. Soc. A* **324**, 301–313 (1971).
- [4] Anh, D. and Shull, K., *Macromolecules* **29**, 4381–4390 (1996).
- [5] Anh, D. and Shull, K., *Langmuir* **14**, 3637–3645 (1998).
- [6] Anh, D. and Shull, K., *Langmuir* **14**, 3646–3654 (1998).
- [7] Léger, L., Raphaël, E., and Hervet, H., *Adv. Polym. Sci.* **138**, 185–225 (1999).
- [8] Vig, J. R., in *Treatise of Clean Surfaces Technology*, K. L. Mittal (Ed.) (Plenum Press, New York, 1987), p. 1.
- [9] Deruelle, M., Hervet, H., Jandeau, G., and Léger, L., *J. Adhesion Sci. Technol.* **12**, 225–247 (1998).
- [10] Amouroux, N., Ph.D. thesis, “Étude des Mécanismes de Modulation de l’Adhérence Entre un Élastomère Silicone et un Adhésif Acrylique,” University Paris VI, Pierre et Marie Curie, 1998.
- [11] Lake, G. and Thomas, A. G., *Proc. R. Soc. Lond. A* **300**, 108–119 (1967).